GEOPHYSICAL RESEARCH LETTERS, VOL. 29, NO. 12, 1610, 10.1029/2001GL014548, 2002

# Large NAT particle formation by mother clouds: Analysis of SOLVE/THESEO-2000 observations

S. Fueglistaler,[1] B. P. Luo,[1] S. Buss,[1] H. Wernli,[1] C. Voigt,[1] M. Müller,[2] R. Neuber,[2] C. A. Hostetler,[3] L. R. Poole,[3] H. Flentje,[4] D. W. Fahey,[5,6] M. J. Northway,[5,6] and Th. Peter[1]

Received 11 December 2001; revised 13 March 2002; accepted 13 March 2002; published 29 June 2002.

[1] During the SOLVE/THESEO-2000 Arctic stratospheric campaign in the winter 1999/2000 widespread occurrences of very large $HNO_3$-containing particles, probably composed of nitric acid trihydrate (NAT), were observed in situ by instruments on board the ER-2 stratospheric research aircraft. These large NAT particles were found with low number densities ($n \approx 10^{-4}$ $cm^{-3}$) in vast regions, in air generally supersaturated with respect to NAT. Within the same campaign other instruments have performed airborne and ground-based measurements of polar stratospheric clouds (PSCs), often showing the existence of type 1a and type 1a-enh clouds. Such PSCs often occur on the mesoscale with particle number densities $n \gtrsim 10^{-2}cm^{-3}$ and are also most likely composed of NAT. We use forward trajectories for the path of NAT particles, which are advected by winds based on ECMWF analyses and sediment due to gravity, to show that high number density NAT PSCs (mother clouds) could give rise to low number density NAT particle populations several days downstream. *INDEX TERMS:* 0305 Atmospheric Composition and Structure: Aerosols and particles (0345, 4801); 0320 Atmospheric Composition and Structure: Cloud physics and chemistry; 0341 Atmospheric Composition and Structure: Middle atmosphere—constituent transport and chemistry (3334)

## 1. Introduction

[2] Ozone destruction is promoted by PSCs in two important ways. First, their surfaces host heterogeneous reactions which cause chlorine activation. Second, PSCs can remove $HNO_3$ through sedimentation, a process termed denitrification. Based on lidar observations by *Browell et al.* [1990], *Toon et al.* [1990] introduced three types of PSCs: type 1a PSCs with low backscatter ratio (BSR) and moderate aerosol depolarization ($\delta_{aerosol}$), which they interpreted as containing small number densities ($n \lesssim 10^{-2}cm^{-3}$ [*Biele et al.*, 2001]) of aspherical particles, most likely nitric acid trihydrate (NAT); type 1b PSCs with moderate BSR and negligible $\delta_{aerosol}$, which were later identified as $\approx$10 $cm^{-3}$ ternary ($HNO_3$/$H_2SO_4$/$H_2O$) aerosol droplets [*Carslaw et al.*, 1994]; and type 2 PSCs with high BSR and $\delta_{aerosol}$ consisting of water ice particles. Later, *Tsias et al.* [1999] identified type 1a-enh PSCs as similar to type 1a but with enhanced NAT particle number densities ($n \gtrsim 0.1$ $cm^{-3}$). During the recent SOLVE/THESEO-2000 Arctic field campaign *Fahey et al.* [2001] discovered extremly large ($r \approx 3-10$ μm) nitric acid hydrate particles, most likely NAT at very low number densities ($n \approx 10^{-4}$ $cm^{-3}$). These so-called "NAT-rocks" play a major role in denitrification which can increase ozone loss.

[3] *Fueglistaler et al.* [2002] and *Dhaniyala et al.* [2002] described a mechanism by which large NAT particles may form from dense NAT clouds ($n \gtrsim 0.01$ $cm^{-3}$) classified as type 1a/1a-enh PSCs. The mechanism, termed by *Fueglistaler et al.* [2002] the "mother cloud/NAT-rock mechanism", comprises the advection of NAT particles within a mother cloud under conditions saturated with respect to NAT ($S_{NAT} \approx 1$) without particle growth, and the subsequent sedimentation of these particles into supersaturated air below the cloud ($S_{NAT} > 1$) where further growth is initiated, consequently leading to large NAT particles in low ($n \approx 10^{-4}$ $cm^{-3}$) number densities. While *Fueglistaler et al.* [2002] and *Dhaniyala et al.* [2002] use idealized models, here different PSC observations during SOLVE/THESEO-2000 are shown to be consistent with the sedimentation of NAT particles based on this mechanism.

## 2. PSC Measurements

[4] We analyzed data from three lidar systems: the ground-based stratospheric aerosol lidar in Ny-Ålesund, Spitsbergen (78.9° N, 11.9° E) operating at two wavelengths (353 nm, 532 nm) [*Beyerle et al.*, 2001]; the NASA LaRC Aerosol Lidar (a piggy-back instrument to the NASA GSFC AROTEL lidar) on board the NASA DC-8 aircraft (532 nm, 1064 nm); and the DLR OLEX lidar system on board the Falcon aircraft (354 nm, 532 nm, 1064 nm) [*Flentje et al.*, 1999]. All three systems measure total backscatter at all wavelengths and depolarization at 532 nm, which allows discrimination between spherical and aspherical (e.g., NAT) particles.

[5] In addition to the lidar data (Figure 1), we use in situ particle measurements from the $NO_y$ instrument on board the NASA ER-2 aircraft [*Fahey et al.*, 2001; *Northway et al.*, 2002]. Two $NO_y$ sampling inlets located on a particle separator body allow *Fahey et al.* [2001] to distinguish large $HNO_3$ containing particles from $NO_y$ in the gas phase and in small particles ($r < 1$ μm). According to the day of measurement, the data is labelled D26, D29 and D31. Similarly, model simulations are labelled S26, S29 and S31.

### 2.1. D26: Ny-Ålesund, Spitsbergen, 26 January 2000

[6] PSCs were observed from the start of the measurements at 03 UTC through the rest of the day (Figure 1a).

[1]Atmospheric and Climate Science, ETH Zürich, Switzerland.
[2]AWI Foundation for Polar and Marine Research, Potsdam, Germany.
[3]NASA Langley Research Center, Hampton, VA, USA.
[4]DLR Oberpfaffenhofen, Wessling, Germany.
[5]NOAA Aeronomy Laboratory, Boulder, CO, USA.
[6]Cooperative Institute for Research in Environmental Sciences, University of Colorado, Boulder, CO, USA.


0094-8276/02/2001GL014548$05.00

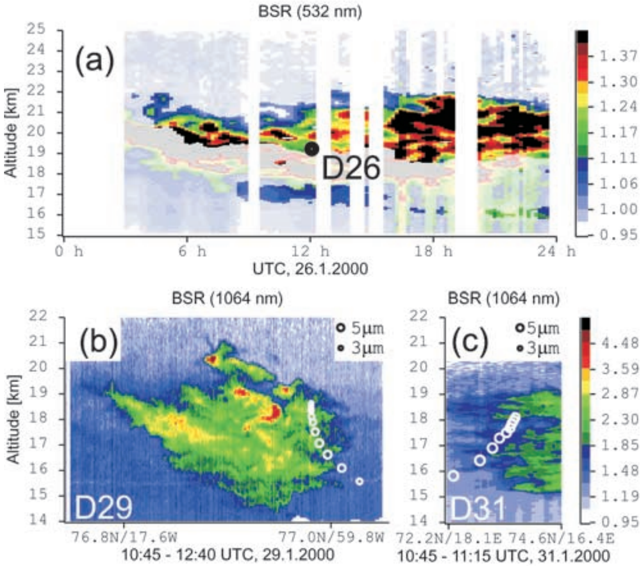


**Figure 1.** (a) D26, Ny-Ålesund ground based lidar on 26 January. Fading colors indicate non-depolarizing signal ($\delta_{aerosol} < 8\%$) from liquid type 1b PSCs. Solid dot: starting point of mother cloud trajectory. (b) D29, LaRC aerosol lidar measurement over Greenland on 29 January. Open circles: location and radius of modelled NAT particles produced by mother cloud trajectory starting at the solid dot in (a). (c) D31, OLEX measurement between North Cape and Spitsbergen on 31 Jan.; particles as in (b).

Using T-Matrix calculations [*Mishchenko*, 1991], the cloud layer at 19–21 km with BSR $\approx$ 1.1–1.7 and $\delta_{aerosol} \approx$ 35–50% can be explained in terms of NAT particles with $n \approx 0.1$–$0.01$ cm$^{-3}$. Backward trajectories calculated with ECMWF (European Center for Medium-Range Weather Forecasts) analysis data of air masses passing Ny-Ålesund at 12 UTC on 26 January reveal a temperature minimum of about 3 K above the ice frost point ($T_{ice}$) 12–24 h earlier when the air passed Greenland. Two days prior to that, the temperatures were well above the NAT existence temperature $T_{NAT}$ (Figure 2a). A numerical hindcast simulation for Greenland with the mesoscale High Resolution Model HRM, initialized at 20 UTC on 25 January, yields lower minimum temperatures around $T_{ice}$ (Figure 2b). This temperature history suggests that the NAT clouds observed over Spitsbergen formed about 12 hours earlier in these cold spots over Greenland, possibly on mesoscale ice clouds. The presence of supercooled ternary solution droplets (STS) below the NAT layer (as indicated by an elevated backscatter without depolarization in Figure 1a) shows that the NAT cloud base is adjacent to air with $S_{NAT} > 1$. This is a necessary condition for NAT particles, sedimenting out of the NAT cloud, to undergo growth below the cloud base. Furthermore, forward air trajectories calculated with ECMWF analysis data from the location of the observed PSCs show that they existed in air masses that remained below $T_{NAT}$ for more than a week (Figure 2a). This could allow the observed NAT PSC to act as a "mother cloud" for large NAT particles [*Fueglistaler et al.*, 2002].

### 2.2. D29: DC-8, Greenland, 29 January 2000

[7] The LaRC aerosol lidar system on board the NASA DC-8 measured a large PSC over Greenland at 14–21 km altitude (Figure 1b, geographical extent shown by the thick black line in Figure 3). Low lidar backscatter, BSR(532 nm) $\leq$1.3, combined with significant aerosol depolarization, $\delta_{aerosol} \approx$ 15–30%, indicates that the cloud consisted of large particles with low number densities. T-matrix calculations [*Mishchenko*, 1991] for aspherical PSC particles [cf.

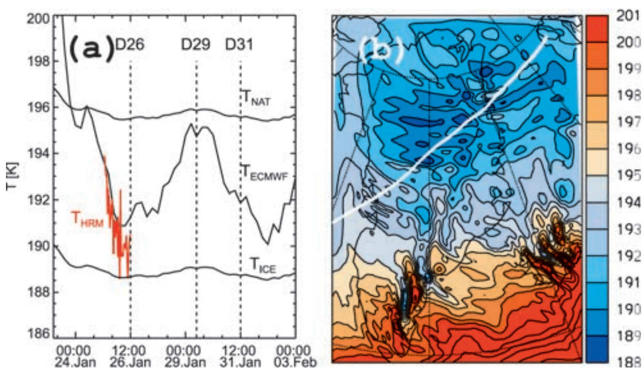


**Figure 2.** (a) Temperature history of air passing over Ny-Ålesund (D26) at 12 UTC on 26 Jan. on the 460 K isentropic surface (approx. 19.3 km altitude). Temperatures from ECMWF (black) and from a mesoscale HRM (red) simulation. NAT and ice existence temperature are calculated with 5.5 ppmv $H_2O$ and 8 ppbv $HNO_3$. D26, D29 and D31 refer to the observations in Figure 1; (b) Temperature at 00 UTC on 26. Jan. on the 460 K isentropic surface from a mesoscale HRM simulation over Greenland. The white line corresponds to the backward trajectory of D26 calculated with HRM data (red line in (a)).

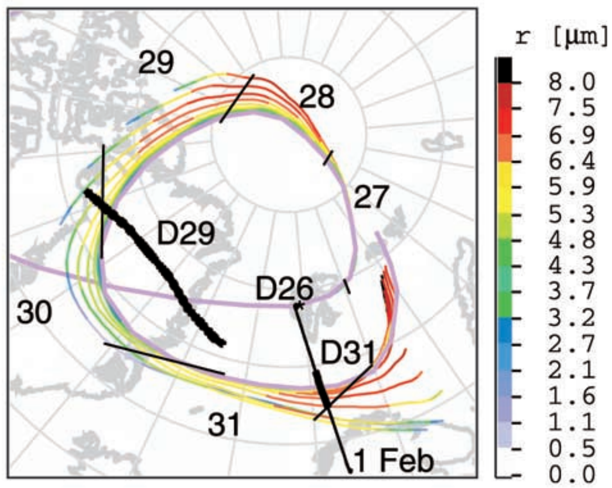


**Figure 3.** Overview of PSC observations and trajectories (air and particles). D26: Ny-Ålesund (ground-based); D29: Greenland (DC-8); D31: North Cape - Spitsbergen (Falcon thick line, ER-2 thin line). Location and date (days of January 2000) shown for 460 K air parcel trajectory (violet) of the mother cloud which was located at 12 UTC on 26 Jan. 2000 over Ny-Ålesund and for sedimenting NAT particle trajectories (color-coded for radius) started along the mother cloud trajectory (see text).

*Carslaw et al.*, 1998] suggest that these observations are best explained as NAT particles with radii $r \geq 3$ μm and number densities $n < 10^{-2}$ cm$^{-3}$.

### 2.3. D31: Falcon and ER-2, North Cape–Spitsbergen, 31 January 2000

[8] On 31 January the Falcon flew from the North Cape to Spitsbergen and back [*Flentje et al.*, 2002]. Due to an iced window, the depolarization data is corrupted over a large portion of the flight, but for the short flight segment presented (Figure 1c) the depolarization data is sound. The observed PSC showed similar depolarization to that seen in the LaRC data from 29 January, but a significantly lower BSR, which indicates an even lower particle number density. The ER-2 flew at the same time as the Falcon (flight track shown in Figure 3). NAT particle populations with number densities of $10^{-4}$ cm$^{-3}$ to as low as $10^{-5}$ cm$^{-3}$ and most probable radii of 4.5–5.5 μm have been inferred from $NO_y$ in situ measurements along broad segments of the flight track [*Northway et al.*, 2002].

## 3. NAT Particle Trajectories

[9] Foreward trajectories of single sedimenting NAT particles were calculated to test the applicability of the mother cloud/NAT-rock mechanism to the observations D26–D31. The equations describing particle growth and sedimentation have been implemented in the trajectory tool LAGRANTO [*Wernli and Davies*, 1997]. The $HNO_3$ vapour pressure of NAT was calculated according to *Hanson and Mauersberger* [1998]. Vortex-averaged gas phase profiles for late January 2000 have been taken from *Schiller et al.* [2002] for $H_2O$ and *Kleinböhl et al.* [2002] for $HNO_3$ and were kept fixed over time (i.e., the gas phase $HNO_3$ depletion between 26 Jan. and 31 Jan. due to the sedimenting NAT particles themselves was ignored). The available $HNO_3$ for NAT particle growth is derived from the equilibrium partitioning of $HNO_3$ into STS [*Carslaw et al.*, 1995]. Particle trajectories with initial particle radius of 1 μm and 3 μm in the mother cloud were calculated to represent the lower and upper limit, respectively, of particle size. In both cases growth and sedimentation were calculated for spherical and aspherical (aspect ratio 1:3) particle shape [*Fueglistaler et al.*, 2002]. As all four cases result in very similar patterns of the sedimenting particle ensemble, concerning size, time and location, only trajectories for spherical particles with an initial radius of 3 μm are presented here (sensitivity studies are shown in the Supplement).

## 4. Results

[10] Figure 3 shows the trajectory of the advected mother cloud (D26) as well as NAT particle trajectories started every 6 hours from 26 January 12 UTC to 31 January 00 UTC from the actual mother cloud position. The match in lat./lon./alt. and time of the particle trajectories with the observations is very good, and calculations (not shown) nearby in time and space to D26 yield similar matches with D29/D31, revealing the robustness of this treatment.

[11] Figure 3 shows that air masses passing over Ny-Ålesund on 26 January 2000 were at the southern edge of a pool of cold air remaining for more than a week below $T_{NAT}$. Note the good agreement of modeled particle positions and the observed end of the PSC at the West coast of Greenland (D29) and at the southern part of D31. To complement Figure 3, in Panels 1b and 1c white circles indicate where particle trajectories intersect with the lidar measurements. Aside from the horizontal (geographical) match, also the vertical extent of the PSCs on 29 and 31 January could be explained by particles sedimenting from the mother cloud.

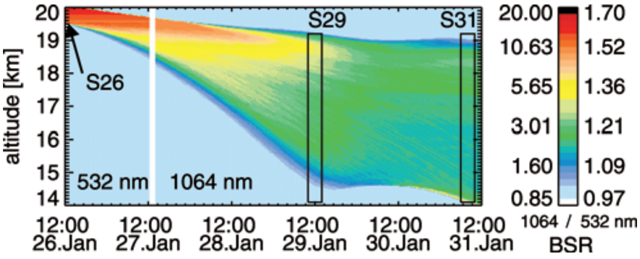


**Figure 4.** Calculated lidar backscatter (left: BSR 532 nm, right: BSR 1064 nm) from a 1-D microphysical model. The mother cloud was initialized with $n$ = 0.01cm$^{-3}$ (corresponding mean particle radius ≈3μm using a log-normal size distribution with σ = 1.2) at an altitude range of 19.5 to 20 km. $HNO_3$ gas phase profile was taken from *Kleinböhl et al.* [2002], $HNO_3$ partitioning into STS is calculated from *Carslaw et al.* [1995]. Temperature profiles are idealized ECMWF profiles taken along the mother cloud trajectory. The data sections labelled S26, S29 and S31 correspond to observations D26, D29 and D31.

[12] From the PSC sedimentation observed by lidar between the outward and incoming flight paths on 31 Jan., *Flentje et al.* [2002] inferred a particle radius of 8 ± 1 μm. Based on in situ measurements of the $NO_y$ instrument, *Northway et al.* [2002] derived particle radii of approximately 5 μm near this location (ER-2 cruise levels ≈ 18 km altitude), remarking that even larger particles ($r \approx$ 10 μm) were observed at 14–15 km altitude. Modelled particle radii of 4 to 7.5 μm at altitudes between 19 and 16 km (Figure 1b, c), respectively, compare well with these observations.

[13] Additional trajectory calculations (see Supplement) show that the eastern part of D29 and the northern part of D31 can be matched with particles sedimenting from a mother cloud located on 26 January 12 UTC about 200–300 km north of Spitsbergen. There are no measurements available at this position, but the similar temperatures of backtrajectories from this location and backtrajectories from D26 support the assumption that the mother cloud observed over Spitsbergen extended 200–300 km further north.

[14] Figure 4 shows the results of a 1-D microphysical model [*Fueglistaler et al.*, 2002]. This model neglects effects caused by wind shear, but takes gas phase depletion from the sedimenting particles into account. This enables accurate calculation of particle sedimentation and particle number densities. The simulation started on 26 Jan. 2000 12 UTC with a mother cloud at 19.5–20 km altitude with $n$ = 0.01 cm$^{-3}$. The vertical temperature profiles over time are idealized ECMWF temperature profiles taken along the mother cloud trajectory. Using T–Matrix calculations, the microphysical data of the model is converted into a simu-

lated lidar backscatter. After ≈3 days, the mother cloud dissolves and after 5 days the sedimenting particle ensemble reaches a particle number density $n \lesssim 10^{-3}\mathrm{cm}^{-3}$ in the entire column. Compared with the measurements D26 (Figure 1a), D29 (Figure 1b) and D31 (Figure 1c), the modelled lidar signals S26, S29 and S31 fit both in absolute BSR and decrease in BSR over time. This is consistent with the assumption that the observed decrease in lidar backscatter resulted from a decrease in particle number density in the PSCs.

## 5. Conclusions and Outlook

[15] PSC observations on 26, 29 and 31 Jan 2000 were matched in latitude, longitude, altitude, and time by forward trajectories of sedimenting NAT particles started from a single advected mother cloud. A 1-D microphysical simulation of particles sedimenting out of the mother cloud reproduces the observed lidar backscatters, and calculated particle radii compare well with in situ measurements. This analysis shows that the suggested mother cloud/NAT-rock mechanism could explain the observed characteristics of large NAT particles without having to invoke a highly selective NAT nucleation mechanism. Instead, the advection of NAT particles within a mother cloud under saturated conditions ($S_{\mathrm{NAT}} \approx 1$) and their subsequent sedimentation into supersaturated regions below the cloud ($S_{\mathrm{NAT}} \gg 1$) with strong growth allows a geographically confined NAT nucleation region to lead to the observed widespread occurrence of large NAT particles far away from the original nucleation area.

[16] As mentioned above, a likely mechanism for the formation of mother clouds is NAT nucleation in ice PSCs. In the Arctic, mountain wave activity over Greenland, Scandinavia and the Urals could lead to enhanced occurrence of ice PSCs [*Carslaw et al.,* 1999]. In the winter 1999/2000, ECMWF analysis data repeatedly showed temperatures below $T_{\mathrm{ice}}$ at altitudes of approximately 19 to 25 km, and reported mountain wave activity led to additional ice PSCs [*Dörnbrack et al.*, 2002]. Thus, frequent occurrence of mother clouds at altitudes of 19 to 25 km can be expected and is in agreement with airborne and ground-based lidar observations of PSCs. *Fueglistaler et al.* [2002] showed that the mother cloud/NAT-rock mechanism requires air parcel temperatures below $T_{\mathrm{NAT}}$ for at least 2 to 3 days to cause significant denitrification. Due to the non-linear particle sedimentation, each additional day greatly enhances the denitrification potential of a mother cloud. *Fueglistaler et al.* [2002] estimated that after 5 days, denitrification amounts up to ≈75% directly below the mother cloud, and significant denitrification extends to ≈4 km below the cloud. Thus, for the winter 1999/2000, a vortex-wide calculation of denitrification based on the mother cloud/NAT-rock mechanism is expected to show denitrification between 16 and 25 km, with a maximum at altitudes around 20 to 22 km. This is in qualitative agreement with observations: In situ $NO_y$ measurements on board the ER-2 show denitrification between 16 and 21 km, with a maximum of up to 80% at 20 to 21 km, and additional balloon-borne data reveal the upper edge of denitirification at about 25 km [*Popp et al.*, 2001].

[17] **Acknowledgments.** We are grateful to C. Schiller and A. Kleinböhl for providing us $H_2O$ and $HNO_3$ data prior to publication. SF and SB have been supported through the EC-project THESEO-2000/EuroSOLVE (under contract BBW 99.0218-2, EVK2-CT-1999-00047) and through an ETHZ-internal research project.

## References

Beyerle, G., et al., Occurrence of solid particles in the winter polar stratosphere above the nitric acid trihydrate coexistence temperature inferred from ground-based polarization lidar observations at Ny-Ålesund, Spitsbergen, *J. Geophys. Res.*, *106*, 2979–2992, 2001.

Biele, J., et al., Nonequilibrium coexistence of solid and liquid particles in Arctic stratospheric clouds, *J. Geophys. Res.*, *106*, 22,991–23,007, 2001.

Browell, E. V., et al., Airborne Lidar Observations In The Wintertime Arctic Stratosphere: Polar Stratospheric Clouds, *Geophys. Res. Lett.*, *17*, 385–388, 1990.

Carslaw, K. S., et al., Stratospheric aerosol growth and $HNO_3$ gas phase depletion from coupled $HNO_3$ and water uptake by liquid particles, *Geophys. Res. Lett.*, *21*, 2479–2482, 1994.

Carslaw, K. S., et al., An analytic expression for the composition of aqueous $HNO_3$-$H_2SO_4$ stratospheric aerosols including gas-phase removal of $HNO_3$, *Geophys. Res. Lett.*, *22*, 1877–1880, 1995.

Carslaw, K. S., et al., Particle microphysics and chemistry in remotely observed mountain polar stratospheric clouds, *J. Geophys. Res.*, *103*, 5785–5796, 1998.

Carslaw, K. S., et al., Widespread solid particle formation by mountain waves in the Arctic stratosphere, *J. Geophys. Res.*, *104*, 1827–1838, 1999.

Dhaniyala, S., et al., Lee-wave clouds and denitrification of the polar stratosphere, *Geophys. Res. Lett.*, *29*(9), 2002.

Dörnbrack, A., et al., Evidence for Inertia-Gravity Waves Forming Polar Stratospheric Clouds over Scandinavia, *J. Geophys. Res.*, in press, 2002.

Fahey, D. W., et al., The Detection of Large $HNO_3$-Containing Particles in the Winter Arctic Stratosphere, *Science*, *291*, 1026–1031, 2001.

Flentje, H., et al., The 3 wavelengths lidar ALEX and other instrumentation onboard the Falcon, ESTEC, Noordwijk, 39–41, ESA WPP-170, ISSN 1022–6656, 1999.

Flentje, H., et al., Denitrification inside the Stratospheric Vortex in the Winter 1999/2000 by Sedimentation of large NAT Particles, *J. Geophys. Res*, in press, 2002.

Fueglistaler, S., et al., NAT-rock Formation By Mother Clouds: A Microphysical Model Study, *Atmos. Chem. Phys. Discuss.*, *2*, 93–98, 2002.

Hanson, D., and K. Mauersberger, Laboratory studies of nitric acid trihydrate: Implications for the south polar stratosphere, *Geophys. Res. Lett.*, *15*(8), 855–858, 1988.

Kleinböhl, A., et al., Vortexwide Denitrification of the Arctic Polar Stratosphere in Winter 1999/2000 determined by Remote Observation, *J. Geophys. Res*, in press, 2002.

Mishchenko, M. I., Light scattering by randomly oriented axially symmetric particles, *J. Opt. Soc. Am.*, *8*, 871–882, 1991.

Northway, M. J., et al., An analysis of large $HNO_3$-containing particles sampled in the Arctic stratosphere during the winter of 1999–2000, *J. Geophys. Res.*, in press, 2002.

Popp, P. J., et al., Severe and Extensive Denitrification in the 1999–2000 Arctic Winter Stratosphere, *Geophys. Res. Lett.*, *28*, 2875–2878, 2001.

Schiller, C., et al., Dehydration in the Arctic stratosphere during the THESEO 2000/SOLVE campaigns, *J. Geophys. Res.*, in press, 2002.

Toon, O. B., et al., An Analysis of Lidar Observations of Polar Stratospheric Clouds, *Geophys. Res. Lett.*, *17*, 393–396, 1990.

Tsias, A., et al., Aircraft lidar observation of an enhanced type Ia polar stratospheric cloud during APE-POLECAT, *J. Geophys. Res.*, *104*, 23,961–23,969, 1999.

Wernli, H., and H. C. Davies, A Lagrangian-based analysis of extratropical cyclones. I: The method and some applications, *Q. J. R. Meteorol. Soc.*, *123*, 467–489, 1997.

S. Fueglistaler, B. P. Luo, S. Buss, H. Wernli, C. Voigt, and Th. Peter, Atmospheric and Climate Science, ETH Zürich, 8093 Zürich, Switzerland. (sf@atmos.umnw.ethz.ch)

M. Müller and R. Neuber, Alfred Wegener Institute Foundation for Polar and Marine Research, Research Unit Potsdam, Telegrafenberg A 43, D-14473, Potsdam, Germany.

C. A. Hostetler and L. R. Poole, NASA Langley Research Center, Hampton, VA, USA.

H. Flentje, DLR Oberpfaffenhofen, 82230 Wessling, Germany.

D. W. Fahey and M. J. Northway, NOAA, Aeronomy Laboratory, Boulder, CO, USA.